2009 American Control Conference
Hyatt Regency Riverfront, St. Louis, MO, USA
June 10-12, 2009

Rotational Angle Based Pressure Control of a Common Rail Fuel Injection System for Internal Combustion Engines

Zhen Zhang and Zongxuan Sun

Abstract— **Common rail based direct injection system is critical for improving the fuel economy and emissions of both gasoline and diesel engines. The fuel pressure pulsation inside the common rail is induced by high-speed flows in and out of the common rail. This phenomenon could adversely affect the accuracy of injected fuel quantities and flow rates. So it is desirable to compensate for the pressure pulsations in a high pressure fuel injection system. Due to the stroke by stroke motion of the internal combustion engine, the fuel pressure pulsation is primarily periodic with respect to the engine rotational-angle since fuel injection timing is scheduled on an angular basis. However, the period of the pressure pulsation changes in time domain as the rotational speed varies in general. To compensate for the pressure pulsations, current control practice is to throttle the fuel through an electro-hydraulic valve, which not only results in energy loss but also has limited effect due to the bandwidth of the valve and the control. In this paper, we apply recently developed time-varying internal model-based design to compensate for the time-varying but angle dependent pressure pulsations.**

I. INTRODUCTION

A precise and flexible fuel injection system is critical to improving vehicle fuel economy and to reducing emissions for both gasoline and diesel engines [1], [2]. Given the immense challenges we are facing for transportation energy, developing efficient, precise, and flexible high-pressure ($2000\,\mathrm{bar}$) and high speed ($80\,\mathrm{mm}^3/\mathrm{ms}$) fuel injection systems will have significant impact on future engines, the transportation industry, and the fluid power industry.

The fuel injection system of internal combustion engines has migrated from a mechanical system to an electronically controlled mechatronic system. The carburetor that is driven mechanically has no flexibility of controlling injection timing and fuel quantity in real-time. The electronic injector that injects into the intake port has some flexibility of adjusting the injection timing, but could not offer multiple injections per engine cycle. The direct injection system, especially the common rail injection system allows the fuel to be injected into the combustion chamber directly at high pressure [1], [3]. This system can control the injection timing and offer multiple injections in real-time according to engine operating conditions. The main control challenge is to further increase the injection pressure and precisely control the injected fuel quantity against the pressure pulsations. Current practice is to control an electro-hydraulic valve to regulate the pressure inside the common rail [4]. Due to the response time of the valve and the bandwidth of the control system, high frequency pulsations cannot be compensated. Also energy loss occurs due to the throttling nature of the electro-hydraulic valve.

The authors are with the Department of Mechanical Engineering, the University of Minnesota, Minneapolis, MN.
Z. Zhang. Email: zhangz@me.umn.edu
Corresponding to: Z. Sun. Phone: 612.625.2107. Email: zsun@umn.edu

Aiming at rejecting the pressure pulsations in the common rail, we propose to design an actuator able to absorb and supply high pressure and high speed flow in real-time to compensate the pressure pulsations. Note that the pressure pulsations are periodic with respect to the engine rotational-angle [5], [6] due to the stroke by stroke motion of the engine operation. To leverage the periodicity of the pressure pulsation in angle domain, we model the system dynamics and design the controller in the angle domain. The difficulty is that the actuator (plant) dynamics becomes time-varying (angel-varying) once it is converted into the angle domain. We show that our recently developed time-varying internal model-based design [7], [8] can be applied to solving this problem. This design has potentials to enable the next generation high-pressure fuel injection system for internal combustion engines.

The paper is organized as follows: In Section II the fundamental pressure dynamics model is introduced. A rotational-angle based control is presented in Section III by first providing the design of a compact and active actuator given in Section III-A, and then using a time-varying internal model-based control for the actuator in Section III-B. The proposed design is validated by simulations presented in Section IV.

II. MODEL OF THE PRESSURE DYNAMICS

In this paper, we consider the problem of controlling the pressure pulsation for a common rail fuel injection system by means of designing an active fluid power storage device and developing a rotational-angle based control algorithm. To begin with, we briefly introduce a common-rail fuel injection system for internal combustion engines. Figure 1 shows the block diagram of a high pressure common-rail fuel injection system, where the main component includes a high pressure pump, a delivery valve, a common rail, an electro-hydraulic valve, and fuel injectors. The high pressure pump generates high-pressure fluid source (up to $2000\,\mathrm{bar}$), which enters the common rail, and the injectors (only one fuel injector is shown in Figure 1) inject high-speed fluid into the combustion chamber. The high-speed flows in and out of the common rail induce pressure pulsations that cause injector metering errors, flow rate variation, and noise [2].

978-1-4244-4524-0/09/$25.00 ©2009 AACC

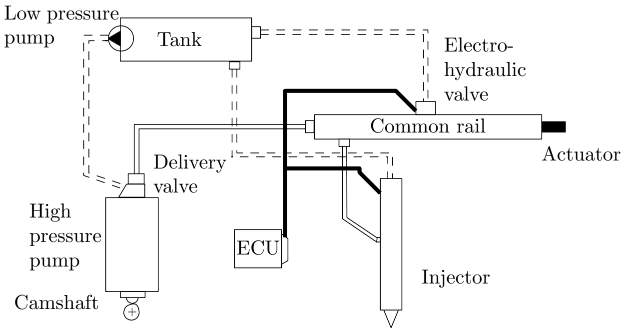

Fig. 1. Block diagram of a common rail fuel injection system [4].

Notation:	
a	model constants
A	output flow section (m^2)
E_k	signals driving k-th injector
$h_{\rm p}$	piston axial displacement (m)
$K_{\rm f}$	fuel bulk modulus of elasticity (bar)
p	real time pressure (bar)
P	constant pressure (bar)
V	volume (m^3)
ω	camshaft speed (rpm)
θ	crankshaft rotational angle (deg)
Subscripts	
cyl	cylinders
i	injectors
r	rail
v	delivery valve
p	pump
t	tank

As shown in [4], the model of the fundamental pressure dynamics due to high-speed flows in a high-pressure environment, where the basic pressure pulsation is caused by high-speed flows, can be characterized as:

$$\begin{aligned}
\dot{p}_{\rm p} &= \tfrac{K_{\rm f}(p_{\rm p})}{V_{\rm p}}(-a_{11}W_{11}\sqrt{p_{\rm p}-P_{\rm t}}-a_{12}W_{12}\sqrt{p_{\rm p}-p_{\rm v}} \\
&\quad +A_{\rm p}\tfrac{dh_{\rm p}}{dt}) \\
\dot{p}_{\rm v} &= \tfrac{K_{\rm f}(p_{\rm v})}{V_{\rm v}}(a_{12}W_{12}\sqrt{p_{\rm p}-p_{\rm v}}-a_{21}\sqrt{p_{\rm v}-p_{\rm r}}) \\
\dot{p}_{\rm r} &= \tfrac{K_{\rm f}(p_{\rm r})}{V_{\rm r}}(a_{21}\sqrt{p_{\rm v}-p_{\rm r}}-a_{31}\textstyle\sum_{k=1}^{n_{\rm i}}\sqrt{p_{\rm r}-p_{{\rm i}k}}- \\
&\quad -u_1\,a_{32}\sqrt{p_{\rm r}-P_{\rm t}}) \\
\dot{p}_{{\rm i}k} &= \tfrac{K_{\rm f}(p_{{\rm i}k})}{V_{\rm i}}(a_{31}\sqrt{p_{\rm r}-p_{{\rm i}k}}-a_{41}\,E_k\,\sqrt{p_{{\rm i}k}-P_{\rm cyl}})
\end{aligned} \tag{1}$$

where the state is the pressure of pump, delivery valve, common rail, and k-th injector, $k=1,\cdots,n_{\rm i}$, with $n_{\rm i}$ the number of injectors, respectively, and input $u_1\in\mathbb{R}$ is the product of the driving current duty cycle and a square signal representing the electro-hydraulic valve activation window. Also W_{11}, $W_{12}=0$, 1 which indicate that some terms in (1) do not exist all the time, for instance $W_{12}=1$ only if the deliver valve is open. Note that for high-pressure and high-speed systems, the wave dynamics also plays a significant role in pressure dynamics, and a simplified wave equation is

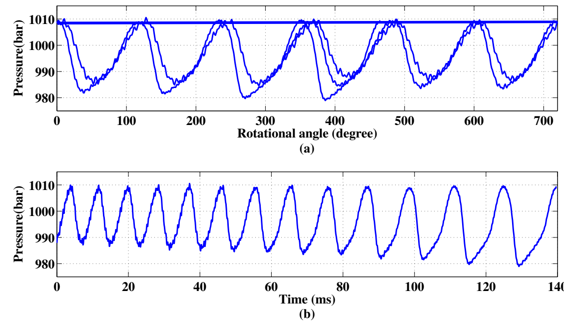

Fig. 2. Common rail pressure pulsation in rotational-angle (a) and time domain (b).

of the form [9]:

$$\frac{\partial^2 p}{\partial z^2}=\frac{1}{c_{\rm s}^2}\frac{\partial^2 p}{\partial t^2} \tag{2}$$

where the direction of flow z, the speed of sound $c_{\rm s}$. Wave dynamics in actual systems is usually much more complex than (2), if the nonlinear effects and thermodynamics are considered, which is out of the scope of this work.

We simulate the fuel injection system model (which is much more complicated than (1)–(2)) in AMESim® (Advanced Modeling Environment for Simulation). From the AMESim® simulation results, it is shown that the basic pressure pulsation is periodic with respect to the internal combustion engine rotational-angle in Figure 2 (a). If the rotational speed is constant, the pressure pulsation is periodic in time domain as well. However, the period of the pressure pulsation changes in real time as the rotational speed varies, as shown in Figures 2 (b). This phenomenon poses a fundamental challenge to suppressing this kind of dynamics [8].

III. Rotational Angle Based Control

As opposite to the current control approach where throttling the fluid through the electro-hydraulic valve only has limited effect because of the bandwidth of the valve, we in this work propose to design an actuator able to absorb and supply high pressure and high-speed flow in real-time so that the pressure pulsations can be suppressed. As the pressure pulsations in the rotational-angle domain is periodic, to leverage this feature of the signal to be rejected, we model the system dynamics and design a controller in the rotational-angle domain as well. It is worth noting that, however, the actuator (plant) dynamics becomes angle-varying when it is converted to the angle domain. We also notice that there are high frequency pressure pulsations in the system caused by the wave dynamics, and this problem is out of the scope of this work but is worth more investigation in the future work.

A. Actuator design

In this section, we design a compact and active fluid power storage device whose bandwidth is wide enough to compensate for the pressure pulsation in the common rail under consideration. To suppress the pressure pulsations, we need a mechanism to absorb and provide high-pressure and

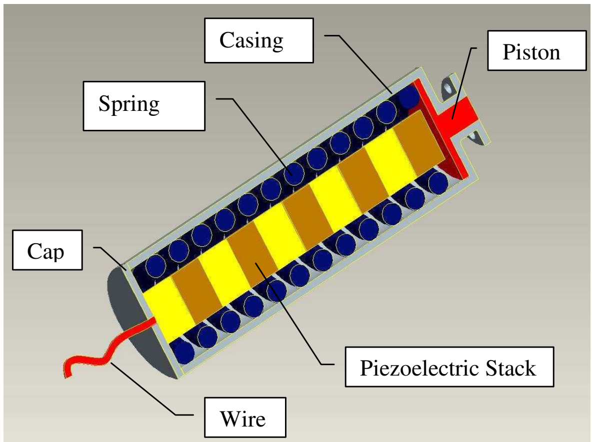

Fig. 3. The design of a compact and active fluid power storage device.

high-speed flows in real-time. As shown in (1), the liquid volume change due to the actuator actuation $\frac{\mathrm{d}v}{\mathrm{d}t}$ must be able to match the intake flow

$$q_{\mathrm{in}} = a_{21}\sqrt{p_{\mathrm{v}} - p_{\mathrm{r}}}$$

and the outtake flow

$$q_{\mathrm{out}} = a_{31}\sum_{k=1}^{n_{\mathrm{i}}}\sqrt{p_{\mathrm{r}} - p_{\mathrm{i}k}} + u_1\, a_{32}\sqrt{p_{\mathrm{r}} - P_{\mathrm{t}}}$$

in order to maintain a steady pressure (say $P_{\mathrm{r}} = 2000\,\mathrm{bar}$).

For example, if the outtake flow $q_{\mathrm{out}} = 80\,\mathrm{mm}^3/\mathrm{ms}$, then we need the actuator be able to account for the volume change $\frac{\mathrm{d}V_{\mathrm{a}}}{\mathrm{d}t} = -80\,\mathrm{mm}^3/\mathrm{ms}$. One possible design of the active fluid power storage device is given in Figure 3, where we adopt a piezoelectric (PZT) stack as the actuator because of its fast response and high stress capability. The maximum stress for the PZT is $130\,\mathrm{mpa}$ and maximum strain is about 1.7% [10]. A few details illustrate the PZT actuator operation: As shown in Figure 3, the actuator consists a case, a piston, a PZT stack and springs. The spring will keep the piston in contact with the case. When high pressure fluid is applied, the piston will overcome the spring force and get in contact with the PZT stack. If the PZT stack is energized, it will contract and the piston will move along with the PZT and increase the fluid volume. If the PZT is energized with opposite polarity, it will push the piston against the fluid pressure and reduce the fluid volume.

B. Control design

With the above actuator, we now develop a trajectory tracking control for the actuator that captures the unique nature of the pressure dynamics to achieve precise and efficient pressure regulation. To take advantage of the periodicity of the reference of the actuator displacement in the rotational-angle domain, we model the system dynamics and design the control method in the rotational-angle domain. However, the actuator (plant) dynamics becomes time-varying [1] when it is converted to the angle domain.

[1]It is indeed angle-varying, here we still call it time-varying and the explanation is given after equation (4).

Since the intake and outtake flows are periodic with respect to the rotational angle (Figure 2 (a)), to compensate the flow induced pressure pulsations, the actuator displacement change $\frac{\mathrm{d}x_{\mathrm{a}}}{\mathrm{d}\theta}$ should be periodic as well by noting that $V_{\mathrm{a}} = A_{\mathrm{a}}x_{\mathrm{a}}$, where A_{a} is the area of the actuator piston. Given the profile of the pressure pulsation Figure 2 (a), it can be shown that the desired actuator displacement d is also periodic in the angle domain. Therefore we need to design a control methodology to track periodic signals for time-varying plant in the rotational-angle domain [7], [8].

In particular, we consider the plant model of the form

$$\begin{array}{rcl} \dot{x}(t) &=& Ax(t) + Bu(t) \\ y(t) &=& Cx(t) \\ e(t) &=& Cx(t) + d(t) \end{array} \tag{3}$$

where plant state $x \in \mathbb{R}^n$, control input $u \in \mathbb{R}$, regulated error $e \in \mathbb{R}$, and reference $d \in \mathbb{R}$. Note that the reference $d(t)$ is periodic with respect to the rotational-angle $\theta(t)$ and $\theta(t)$ is defined as $\theta(t) := \varphi(t) = \int_{t_0}^{t}\omega(\tau)d\tau$, assuming $\varphi(t_0) = 0$ with the rotational speed $\omega(t) > 0$. Then reference $d(t)$ in θ domain reads as $d(t) = d(\varphi^{-1}(\theta)) = \bar{d}(\theta) = \bar{d}(\theta + \Theta)$, with a constant $\Theta > 0$. In order to leverage the periodicity of the $\bar{d}(\cdot)$, we convert the plant model (3) into the rotational-angle domain [11] as:

$$\begin{array}{rcl} \frac{\mathrm{d}\bar{x}(\theta)}{\mathrm{d}\theta} &=& \frac{1}{\bar{\omega}(\theta)}A\bar{x}(\theta) + B\frac{1}{\bar{\omega}(\theta)}\bar{u}(\theta) \\ \bar{y}(\theta) &=& C\bar{x}(\theta) \\ \bar{e}(\theta) &=& C\bar{x}(\theta) + \bar{d}(\theta) \end{array} \tag{4}$$

with $\bar{x}(\theta) := x(\varphi^{-1}(\theta))$, $\bar{y}(\theta) := y(\varphi^{-1}(\theta))$, $\bar{u}(\theta) := u(\varphi^{-1}(\theta))$, and $\bar{\omega}(\theta) := \omega(\varphi^{-1}(\theta))$. Clearly the actuator model (4) is linear angle-varying but not periodically angle-varying if $\bar{\omega}(\cdot)$ is not periodic in θ. When no confusion occurs, we still call system (4) linear time-varying as system (4) remains same when the independent variable θ is replaced by t. It can be shown that if system (3) is controllable and observable, then system (4) is uniformly controllable and observable. For implementation, we sample system (3) at $\theta(0), \theta(1), \cdots, \theta(k), \cdots$, and the corresponding zero-order-hold sampling of the system, in the rotational-angle domain, is of the form:

$$\begin{array}{rcl} x(k+1) &=& F(k)x(k) + G(k)u(k) \\ e(k) &=& H(k)x(k) + d(k) \end{array} \tag{5}$$

where $k+1$ denotes the time $t = t_{k+1}$ at the sampling instant $\theta(k+1)$ with the varying sampling time $T(k) := t_{k+1} - t_k = \frac{\theta(k+1)-\theta(k)}{\omega(k)}$, and $F(k) = e^{AT(k)}$ with $G(k) = (e^{AT(k)} - I)A^{-1}B$, when matrix A is invertible.

In order to apply our recently developed controller design via I/O representation, we transform the state space model (5) to polynomial fraction representation. To do so, we briefly introduce the definitions on polynomial delay operator (PDO) and polynomial summation operator (PSO) (see [7], [12]).

Definition 3.1: Denote the one step delay operator z^{-1}. The left polynomial delay operator (PDO) of degree n, $P(z,k)$, is defined as:

$$P(z,k) = a_n(k)z^{-n} + \cdots + a_1(k)z^{-1} + a_0(k)\,,$$

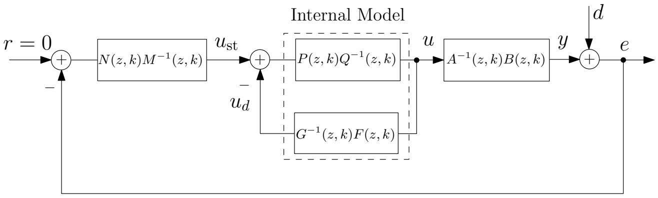

Fig. 4. Internal model-based controller.

and likewise, the right PDO of degree n is defined as:

$$\bar{P}(z,k) = z^{-n}\bar{a}_n(k) + \cdots + z^{-1}\bar{a}_1(k) + \bar{a}_0(k)\,,$$

where $a_i(k)$ and $\bar{a}_i(k)$, $i = 0, \cdots, n$, are bounded functions of k and $a_n(k) \neq 0$, $\bar{a}_n(k) \neq 0$, for some $k \geq 0$. If $a_0(k) = 1$ ($\bar{a}_0(k) = 1$), for all k, the above left (right) PDO is termed as *monic*.

Definition 3.2: A left (right) polynomial summation operator (PSO) of order n, $P^{-1}(z,k)$, is defined as the operator that maps the input u to the zero state response of the difference equation $P(z,k)[y] = u$, where $P(z,k)$ is a monic left (right) (PDO).

By definition of PSO, it is natural to consider its stability as introduced in Definition 3.3.

Definition 3.3: A PSO, $P^{-1}(z,k)$, is said to be exponentially stable (ES), if and only if there exists a finite positive constant κ and a constant $0 \leq \mu < 1$ such that the state transition matrix $\Phi(i,j)$, associated with the linear differential equation $P(z,k)[y] = 0$, satisfies

$$\|\Phi(i,j)\| \leq \kappa\,\mu^{i-j}\,, \quad \text{for all } i \geq j\,.$$

It can be shown [7] that by means of $A^{-1}(z,k)B(z,k) = H(k)(zI - F(k))^{-1}G(k)$, the I/O representation of system (5) is put in the form

$$e(k) = A^{-1}(z,k)B(z,k)[u(k)] + d(k)\,, \tag{6}$$

where $B(z,k)$ is a PDO and $A^{-1}(z,k)$ is an ES PSO which is guaranteed if the spectrum of A in (3) lies in the open left hand side complex plane. The reference $d(k)$ to be tracked satisfies the model of the form

$$\Lambda(z)[d] = (1 - z^{-N})[d] = 0\,, \tag{7}$$

with a time-invariant PDO $\Lambda(z)$.

The control structure we adopted in this work is shown in Figure 4. The main idea behind the structure is that a time-varying (as the plant is time-varying) internal model unit has to be designed to reconstruct the exogenous signal d.

We recall our recent developed results for the time-varying tracking control design.

Proposition 3.1: [8] Consider plant model (6) and exogenous signal model (7). If PDO $P(z,k)$, $Q(z,k)$, $N(z,k)$ and $M(z,k)$ satisfy the following conditions:

$$A(z,k)Q(z,k) + B(z,k)P(z,k) = \Lambda(z)Q(z,k) \tag{8}$$

$$\Lambda(z)Q(z,k)\bar{M}(z,k) + B(z,k)P(z,k)\bar{N}(z,k) = A_s(z,k) \tag{9}$$

where $A_s^{-1}(z,k)$ is an ES PSO, and

$$\begin{aligned} \bar{M}(z,k) &= Q^{-1}(z,k)M(z,k) \\ \bar{N}(z,k) &= Q^{-1}(z,k)N(z,k)\,, \end{aligned}$$

the asymptotic performance is achieved, i.e.,

$$\lim_{k\to\infty} e(k) = 0\,.$$

IV. SIMULATION

Consider the plant (piezoelectric actuator) model (3) with plant state $x \in \mathbb{R}^2$, the axial displacement and the velocity of the piston on the actuator, control input $u \in \mathbb{R}$, the PZT thrust force, regulated displacement error $e \in \mathbb{R}$, and displacement reference $d \in \mathbb{R}$, and

$$A = \begin{pmatrix} 0 & 1 \\ -\frac{k_{\text{s}}}{m_{\text{a}}} & -\frac{b}{m_{\text{a}}} \end{pmatrix}\,, \quad B = \begin{pmatrix} 0 \\ \frac{1}{m_{\text{a}}} \end{pmatrix}\,, \quad C = \begin{pmatrix} 1 & 0 \end{pmatrix}$$

with m_{a} the total moving mass, b the damping constant, k_{s} the effective spring rate. The actuator displacement profile $d(t)$ is periodic in the rotational-angle domain, and it satisfies the model $d(\theta + k2\pi/n_{\text{i}}) = d(\theta)$, with an integer k and the number of injectors n_{i}. Put the above system into the form (5). It can be shown that the corresponding I/O representation of system (5) is of the form (6), where

$$A(z,k) = 1 + z^{-1}a_1(k) + z^{-2}a_2(k)\,,$$

with

$$\begin{aligned} a_1(k) &= -f_{11}(k) - \frac{f_{12}(k)}{f_{12}(k-1)}f_{22}(k-1) \\ a_2(k) &= \frac{f_{12}(k+1)}{f_{12}(k)}f_{11}(k)f_{22}(k) - f_{12}(k+1)f_{21}(k)\,, \end{aligned}$$

and

$$B(z,k) = z^{-1}b_1(k) + z^{-2}b_2(k)\,,$$

with

$$\begin{aligned} b_1(k) &= g_1(k) \\ b_2(k) &= -\tfrac{f_{12}(k+1)}{f_{12}(k)}g_1(k)f_{22}(k) + f_{12}(k+1)g_2(k)\,. \end{aligned}$$

Note that the preview term $f_{12}(k+1)$ is superfluous, as it only occurs in the right side of z^{-2} and hence one can avoid this in implementation by using left polynomial operators and $f_{12}(k) \neq 0$ for the range of $T(k)$.

Now we are in position to design the LTV controllers to satisfy the conditions (8)– (9). Given the waveform of the pressure pulsation in the rotational-angle domain (see Figure 2 (a)), we sample the signal d four times in every $1/6$ engine cycle (for the v6 engine), i.e., there are 6 injections per one engine cycle. Therefore the reference model is of the form

$$\Lambda(z) = 1 - z^{-4}\,.$$

Step 1: Solve $P(z,k)$ and $Q(z,k)$ to satisfy condition (8). Let

$$\begin{aligned} Q(z,k) &= 1 + z^{-1}q_1(k) \\ P(z,k) &= p_0(k) + z^{-1}p_1(k) + z^{-2}p_2(k) + z^{-3}p_3(k)\,, \end{aligned}$$

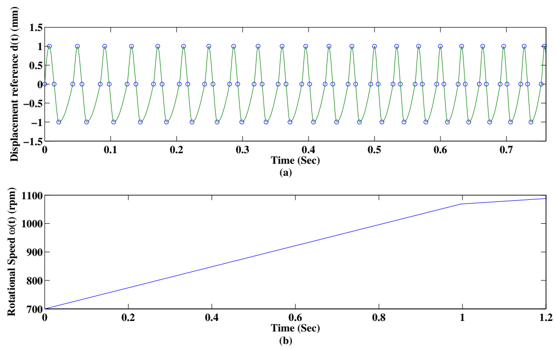

Fig. 5. Actuator displacement reference and rotational speed in time domain.

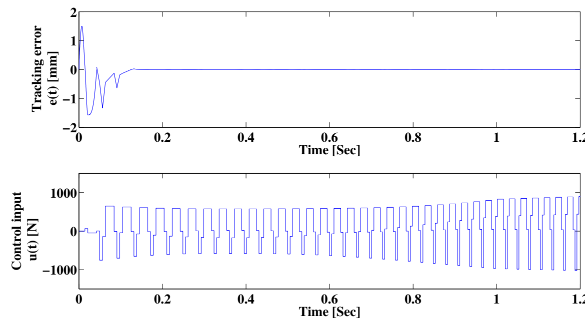

Fig. 6. Tracking error and control input.

and substitute them into (8) yielding:

$$(1+z^{-1}a_1(k)+z^{-2}a_2(k))(1+z^{-1}q_1(k))+(z^{-1}b_1(k)+ \\ +z^{-2}b_2(k))(p_0(k)+z^{-1}p_1(k)+z^{-2}p_2(k)+z^{-3}p_3(k)) = \\ (1-z^{-4})(1+z^{-1}q_1(k))\,.$$

The corresponding Diophantine equation admits the following realization

$$S(k)\phi(k)=\beta(k)\,,$$

where

$$\phi(k)=\mathrm{col}(q_1(k),p_0(k),p_1(k),p_2(k),p_3(k))\,,$$
$$\beta(k)=\mathrm{col}(a_1(k),a_2(k),0,-1,0)\,,$$

and

$$S(k)= \begin{pmatrix} 0 & b_1(k) & 0 & 0 & 0 \\ a_1(k+1) & b_2(k) & b_1(k+1) & 0 & 0 \\ a_2(k+1) & 0 & b_2(k+1) & b_1(k+2) & 0 \\ 0 & 0 & 0 & b_2(k+2) & b_1(k+3) \\ 1 & 0 & 0 & 0 & b_2(k+3) \end{pmatrix}.$$

Step 2: Solve $\bar{N}(z,k)$ and $\bar{M}(z,k)$ to meet condition (9). By choosing

$$\begin{aligned} \bar{N}(z,k) &= n_0(k)+z^{-1}n_1(k)+\cdots+z^{-4}n_4(k) \\ \bar{M}(z,k) &= 1+z^{-1}m_1(k)+\cdots+z^{-4}m_4(k)\,, \end{aligned}$$

and $A_s(z,k)=(1+(c\,z)^{-1})^9$, with $|c|>1$, equation (9) reads as:

$$(1-z^{-4})(1+z^{-1}q_1(k))(1+z^{-1}m_1(k)+z^{-2}m_2(k) \\ +z^{-3}m_3(k)+z^{-4}m_4(k))+(z^{-1}b_1(k)+z^{-2}b_2(k))(p_0(k) \\ +z^{-1}p_1(k))(n_0(k)+z^{-1}n_1(k)+z^{-2}n_2(k)+z^{-3}n_3(k) \\ +z^{-4}n_4(k))=(1+(c\,z)^{-1})^9\,.$$

The matrix realization is similar to that in Step 1, and hence is omitted.

It is shown in Figure 5 (a) that the reference of the actuator displacement is not periodic (sampled data are marked in dot) in time domain as the engine speed varies shown in Figure 5 (b). To validate the proposed algorithm, the rotational speed profile is selected from the Federal Testing Procedure (FTP) data. The regulated error and control input are shown in Figure 6, where asymptotic performance has been achieved and the control input is not periodic as expected.

V. Conclusions

We have considered the pressure regulation problem in a high pressure fuel injection system, as the current control method by means of throttling the electro-hydraulic valve not only leads to energy loss but also has limited effect due to the bandwidth of the valve and the control. To achieve more desirable fuel injection performance, by leveraging the periodicity of pulsation in rotational-angle domain, we design an actuator capable of absorbing and providing high pressure and high speed flow in real time. As a result, plant dynamics becomes time-varying and we have shown that how our recently developed time-varying internal model-based design can be applied to the injection pressure regulation for the common rail fuel injection system.

In the future work, the construction of a robust controller, in the sense that the knowledge of the original LTI plant model is only available up to certain bandwidth, is under investigation. Also the wave dynamics of the fuel injection system needs to be better understood so that it can be used to guide the positioning of the PZT actuator.

References

[1] N. Guerrassi and P. Dupraz. A common rail injection system for high speed direct injection diesel eninges. *SAE*, 1998-08-03, 1998.

[2] Q. Hu, S.F. Wu, S. Stottler, and R. Raghupathi. Modelling of dynamic responses of an automotive fuel rail system, part I: Injector. *Journal of Sound and Vibration*, 245(5):801 – 814, 2001.

[3] G. Stumpp and M. Ricco. Common rail-an attractive fuel injection system for passenger car DI diesel engines. *SAE paper 960870*, 1986.

[4] P. Lino, B. Maione, and A. Rizzo. Nonlinear modeling and control of a common rail injection system for diesel eninges. *Applied Mathematical Modeling*, 31:1770–1784, 2007.

[5] Y. K. Chin and F.-E. Coats. Engine dynamics: Time-based versus crank-angle based. In *SAE Technical Paper Series 860412*, 1986.

[6] S. Yurkovich and M. Simpson. Comparative analysis for idle speed control: A crank-angle domain viewpoint. volume 1, pages 278 – 283, Albuquerque, NM, USA, 1997.

[7] Z. Sun. Tracking or rejecting rotational-angle dependent signals using time varying repetitive control. In *Proceeding of the 2004 American Control Conference*, pages 144–149, Boston, MA, 2004.

[8] Z. Sun, Z. Zhang, and T. C. Tsao. Trajectory tracking and disturbances rejection for linear time-varying systems: input/output representation. Systems & Control Letters, in press, 2009.

[9] G. J. Sharpe. *Solving Problems in Fluid Dynamics*. Harlow, Essex, England: Longman Scientific and Technical; New York: Wiley, 1994.

[10] S. Park and T. Shroul. Ultrahigh strain and piezoelectric behavior in relaxor based ferroelectric single crystals. *Journal of Applied Physics*, 82:1804–1811, 1997.
[11] C.-L. Chen and G. T.-C. Chiu. Spatially periodic disturbance rejection with spatially sampled robust repetitive control. *Journal of Dynamic Systems, Measurement, and Control*, 130(2):021002, 2008.
[12] K. S. Tsakalis and P. A. Ioanou. *Linear Time-Varying Systems: Control and Adaptation*. Advances in Industrial Control. Prentice Hall, Englewood Cliffs, NJ, 1993.